Sine-Transform-Based Memristive Hyperchaotic Model With Hardware Implementation

Han Bao, *Member, IEEE*, Houzhen Li, *Graduate Student Member, IEEE*, Zhongyun Hua, *Member, IEEE*, Quan Xu, *Member, IEEE*, and Bocheng Bao, *Member, IEEE*

***Abstract*—Memristor is a special nonlinear circuit component with internal state and can lead to excellent chaos complexity in its constructed discrete system. To enhance the chaos complexity of a memristor-based discrete system, this article proposes a 2-D sine-transform-based (STB) memristive model. The model has line fixed point and its stability is dependent on memristor initial state. Complex dynamics with quasi-periodic bifurcation and multistability are demonstrated using numerical methods. For different control parameters, chaotic and hyperchaotic attractors are emerged and their complicated fractal structures and outstanding performance indicators are exhibited. A hardware prototype is developed and these attractors are experimentally captured therein. Besides, six pseudorandom number generators (PRNGs) are designed using the proposed model under different control parameters and the test results by the TestU01 standard show that these PRNGs have high randomness without chaos degradation. In brief, the proposed 2-D STB memristive model is flexible to generate chaos and hyperchaos with high performance.**

***Index Terms*—Chaos, chaos degradation, control parameter, hyperchaos, line fixed point, memristor, pseudorandom number generator (PRNG), sine transform.**

I. Introduction

Chaos is a kind of nonlinear phenomenon and some chaos phenomena can be described by definite mathematical models. A chaotic system can generate bounded chaos and has many excellent characteristics, such as initial sensitivity, random similarity, and track ergodicity [1]. With these characteristics, chaotic systems are widely used in many industrial applications [2]–[4]. To produce chaos, at least one nonlinear term is required in a dynamical system. The widely used nonlinear term include polynomial function, trigonometric function, hyperbolic tangent function, exponential function, etc. These nonlinear terms can be realized using some commercial circuit components [5]. However, they do not involve any internal states. With internal state, memristor is a special nonlinear circuit component and is different from these widely used nonlinear terms in nature [6]. This special nonlinearity makes memristors popularly used for designing chaotic oscillation circuits and neuromorphic networks [7]–[10].

Recently, chaos estimation technology has been rapidly developed with the fast improvement of computing ability. Due to the limited performance, many chaotic systems were demonstrated to be inadequate in some practical applications [11]. Using artificial intelligence technologies, the chaotic behaviors of some chaotic systems can be effectively predicated by directly predicting the chaotic sequences, or estimating the control parameters and initial states [12]–[14]. On the other hand, many chaotic systems show weak chaos, which indicates that the chaotic behaviors are not robust and small changes in the control parameters may lead to chaos degradation [15]. Furthermore, with simple algebraic structures and dynamical behaviors, the dynamical degradation is often encountered in many chaotic systems, resulting in serious security issues [16], [17]. Therefore, it is of great significance to develop chaotic systems with strong ability to avoid chaos degradation.

Hyperchaos is a more complex dynamical behavior than chaos, since it has at least two positive Lyapunov exponents (LEs). Thus, hyperchaotic sequences show high security level for many practical applications, such as secure video/RM-DCSK communication [18], [19]. To acquire hyperchaos, a continuous system requires at least four dimensions, whereas a discrete system requires only two. For example, discrete memristor-coupled Logistic map [20], nonautonomous memristor-based map [21], and sine chaotification map [22] are all 2-D discrete systems and they can display hyperchaos. By introducing memristor nonlinearities or chaotification schemes, several discrete hyperchaotic systems have been presented in recent years [23]–[26]. On the one hand, a 2-D sine chaotification discrete system was proposed in [22] to improve the chaos complexity of existing 2-D discrete chaotic systems. On the other hand, a general framework for 2-D memristive hyperchaotic systems was constructed in [19] by coupling discrete memristor with cosine memductance to some 1-D discrete systems, and a general 3-D memristor mapping model was proposed in [23] by coupling this discrete memristor to four 2-D discrete maps. The analysis results show that the

Manuscript received 2 January 2022; revised 21 February 2022; accepted 2 March 2022. Date of publication 7 March 2022; date of current version 3 March 2023. This work was supported in part by the National Natural Science Foundations of China under Grant 12172066, Grant 62071142, and Grant 51777016 and in part by the Natural Science Foundation of Jiangsu Province, China, under Grant BK20191451. Paper no. TII-22-0005. *(Corresponding author: Bocheng Bao.)*

Han Bao, Houzhen Li, Quan Xu, and Bocheng Bao are with the School of Microelectronics and Control Engineering, Changzhou University, Changzhou 213164, China (e-mail: charlesbao0319@gmail.com; leehzh@126.com; xuquan@cczu.edu.cn; baobc@cczu.edu.cn).

Zhongyun Hua is with the School of Computer Science and Technology, Harbin Institute of Technology, Shenzhen, Shenzhen 518055, China (e-mail: huazhongyun@hit.edu.cn).

Color versions of one or more figures in this article are available at https://doi.org/10.1109/TII.2022.3157296.

Digital Object Identifier 10.1109/TII.2022.3157296

memristor can greatly enhance the chaos complexity of these existing discrete systems. Meanwhile, a memristive Rulkov neuron model was established successfully in [24] by importing discrete memristor with hyperbolic tangent memductance into a 2-D Rulkov neuron model. The memristive Rulkov neuron model showed the memristor-induced magnetic induction effect and memristor initial state-dependent extreme multistability. In addition, because of simple algebraic structures, the computational efficiency of the discrete systems is much higher than that of the continuous systems in practical applications [22]. Then, designing discrete hyperchaotic systems with simple algebraic structures is also an interesting topic. Thus, it is of great interest to design discrete hyperchaotic systems owing outstanding performance without chaos degradation by combining memristor nonlinearity with simple chaotification scheme.

By combining the memristor nonlinearity with the sine transform scheme used in [22], this article proposes a novel 2-D sine-transform-based (STB) memristive model to generate chaotic and hyperchaotic attractors. The novelty and main contributions of this article are summarized as follows.

1) We propose a novel 2-D STB memristive model with line fixed point and explore its complex dynamical behaviors with quasi-periodic bifurcation and muiltistability.
2) Using different control parameters, different chaotic and hyperchaotic attractors are emerged from the memristive model and they are experimentally captured by a digital hardware prototype.
3) Performance analyses show that these chaotic and hyperchaotic attractors have complicated fractal structures and outstanding performance indicators.
4) Six pseudorandom number generators (PRNGs) are designed using the proposed model under different control parameters and the test results by the TestU01 show their high randomness without chaos degradation.

The rest of this article is organized as follows. Section II proposes a 2-D STB memristive model. Section III studies the control parameter-related dynamical behaviors and displays the chaotic and hyperchaotic attractors. The generated chaotic/hyperchaotic sequences are evaluated and compared in Section IV. The hardware experiments are carried out and the designed PRNGs are tested by the TestU01 in Section V. Finally, Section VI concludes this article.

II. 2-D STB Memristive Model

This section presents the 2-D STB memristive model, and discusses its line fixed point and stability dependent on the memristor initial state.

A. Schematic Structure and Mathematical Model

Memristor is a special nonlinear circuit component with internal state. According to the discrete mathematical representation of memristor in [25], an ideal charge-controlled memristor can be described by

$$\begin{aligned} v_n &= M(q_n) i_n \\ q_{n+1} &= q_n + i_n \end{aligned} \tag{1}$$

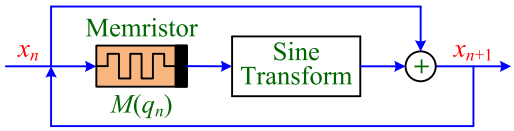

Fig. 1. Schematic structure of the general STB memristive model.

where v_n, i_n, and q_n are the values of output $v(t)$, input $i(t)$, and internal state $q(t)$ at the nth iteration, respectively, and $M(q_n)$ is the value of memristance $M(q)$ at the nth iteration.

Using the discrete memristor in (1), a simple implementation approach of generating 2-D discrete memristor maps was proposed in [25] and four 2-D discrete memristor hyperchaotic maps were provided. However, these discrete memristor maps have simple algebraic structures and their short-term behaviors may be estimated using some artificial intelligence techniques [1]. Chaotification schemes can be used to further increase the chaos complexity of these discrete memristor maps. To this end, a simple chaotification scheme is used as a nonlinear function to transform the output of discrete memristor for further improving their chaos performance.

The schematic structure of a general STB memristive model is shown in Fig. 1. The input x_n is fed into the memristor, and then nonlinear transformation is implemented for the memristor output by sine transformation. The general STB memristive model can be mathematically described as

$$\begin{cases} x_{n+1} = x_n + a \sin[\pi M(q_n) x_n] \\ q_{n+1} = x_n + q_n \end{cases} \tag{2}$$

where a is a positive control parameter.

The quadratic memductance nonlinearity reported in [25] is taken as an example and it is expressed as

$$M(q_n) = q_n^2 - b \tag{3}$$

where b is another positive control parameter.

Substituting (3) into (2), a specific STB memristive model is thereby yielded as

$$\begin{cases} x_{n+1} = x_n + a \sin[\pi(y_n^2 - b) x_n] \\ y_{n+1} = x_n + y_n \end{cases} \tag{4}$$

where a linear transformation $q \to y$ is used. Thus, the STB memristive model in (4) is a 2-D discrete system with two control parameters a and b, and its dynamical behaviors are determined by the two control parameters.

The STB memristive model in (4) contains an STB memristor, which is described by

$$\begin{aligned} v_n &= \sin[\pi(q_n^2 - b) i_n] \\ q_{n+1} &= q_n + i_n. \end{aligned} \tag{5}$$

Thus, the STB memristor is a generalized memristor and it is different from the ideal memristor described in (1). When applying $i_n = 0.04\sin(\omega n)$ A (ω is radian frequency) to the STB memristor, the pinched hysteresis loops are generated, as depicted in Fig. 2. Consequently, the STB memristor can show the radian frequency/initial state-dependent pinched hysteresis

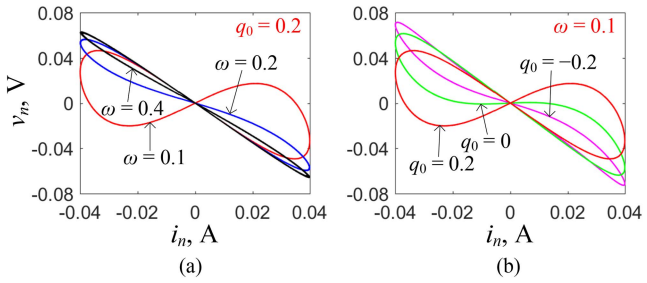

Fig. 2. Pinched hysteresis loops of the STB memristor when applying $i_n = 0.04\sin(\omega n)$ A. (a) Radian frequency-dependent fingerprints for fixed $q_0 = 0.2$ C. (b) Initial state-dependent fingerprints for fixed $\omega = 0.1$ rad/s.

loops, demonstrating that it can also satisfy the fingerprints of generalized memristor [6].

B. Line Fixed Point and Stability

A fixed point of a mapping model is an element of the model's domain that maps to itself. The fixed point of the 2-D STB memristive model can be obtained by solving the following equations:

$$\begin{cases} X = X + a\sin[\pi X(Y^2 - b)] \\ Y = X + Y \end{cases}. \tag{6}$$

Obviously, the proposed model has a line fixed point and the line fixed point is described by

$$S = (X, Y) = (0, \mu) \tag{7}$$

where μ is an arbitrary constant, representing the initial state of the memristor.

The fixed point is stable or unstable and its stability is characterized by the eigenvalues of the model's Jacobian matrix at that point. The Jacobian matrix of the 2-D STB memristive model at S is given by

$$\mathbf{J}_S = \begin{bmatrix} 1 + \pi a(\mu^2 - b) & 0 \\ 1 & 1 \end{bmatrix}. \tag{8}$$

Correspondingly, the characteristic polynomial equation is calculated as

$$P(\lambda) = (\lambda - 1)[\lambda - 1 - \pi a(\mu^2 - b)] \tag{9}$$

and two eigenvalues λ_1 and λ_2 are calculated as

$$\lambda_1 = 1, \lambda_2 = 1 + \pi a(\mu^2 - b). \tag{10}$$

If λ_1 and λ_2 are both inside the unit circle, the proposed model is stable; otherwise, it is unstable. It can be observed from (10) that λ_1 is always on the unit circle, i.e., λ_1 is critically stable, whereas λ_2 could be outside or inside the unit circle, i.e., the proposed model can be unstable or critically stable, depending on the control parameters a and b as well as the memristor initial state μ. When a and b are specified, the critically stable interval of μ can be derived from (10) as

$$\mu \in \left(-\sqrt{b}, \sqrt{b}\right) \tag{11}$$

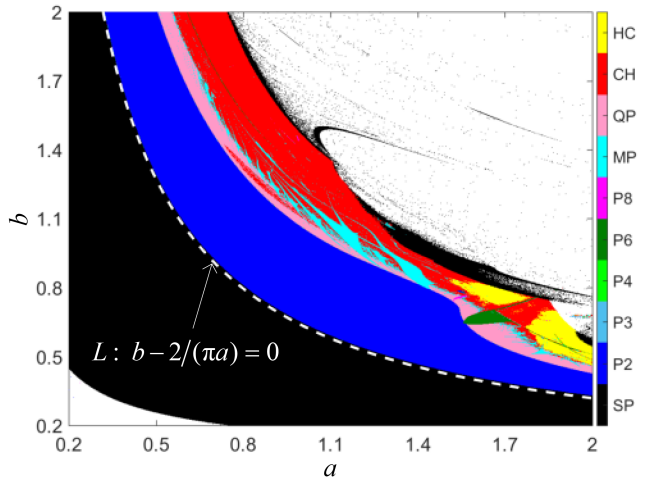

Fig. 3. 2-D mixed bifurcation plot in the $a - b$ parameter plane under the initial states $(x_0, y_0) = (0.1, 0.1)$.

for $b < 2/(\pi a)$ or

$$\mu \in \left(-\sqrt{b}, -\sqrt{b - 2/(\pi a)}\right) \cup \left(\sqrt{b - 2/(\pi a)}, \sqrt{b}\right) \tag{12}$$

for $b > 2/(\pi a)$. This implies that the 2-D STB memristive model may be critically stable when the memristor initial state μ satisfies the critically stable condition given in (11) or (12).

In summary, the proposed 2-D STB memristive model has line fixed point and its stability depends on the control parameters and memristor initial state. Therefore, the proposed 2-D STB memristive model is prone to multistability owning to the memristor initial state-dependent stability [19].

III. Dynamical Behaviors and Strange Attractors

This section studies control parameter-related dynamical behaviors of the 2-D STB memristive model in terms of mixed bifurcation plots, phase plane attractors, and basins of attraction. The initial states of the proposed model are set as fixed values, i.e., $(x_0, y_0) = (0.1, 0.1)$.

A. Dynamical Behaviors Depicted by Bifurcation Plots

By measuring the iterative periodicities and LEs of a discrete map, a colorful 2-D mixed bifurcation plot can be depicted in the parameter plane. The LEs are computed using Wolf's Jacobian-based method. Fig. 3 shows the 2-D mixed bifurcation plot of the 2-D STB memristive model with $a \in [0.2, 2]$ and $b \in [0.2, 2]$. The parameter plane regions triggering the motion trajectories with different iterative periodicities are pained using different colors. The yellow, red, and pink areas represent hyperchaos (labeled HC), chaos (labeled CH), and quasi-period (labeled QP), respectively; the black, cyan, and white areas represent stable point (labeled SP), multiperiod (labeled MP), and unbounded behavior, respectively; other color areas represent period-2 to period-8 (labeled P2 to P8). It is clear that the colors have the transition from blue (period-2) to pink (quasi-period), leading to the quasi-periodic bifurcation route to chaos

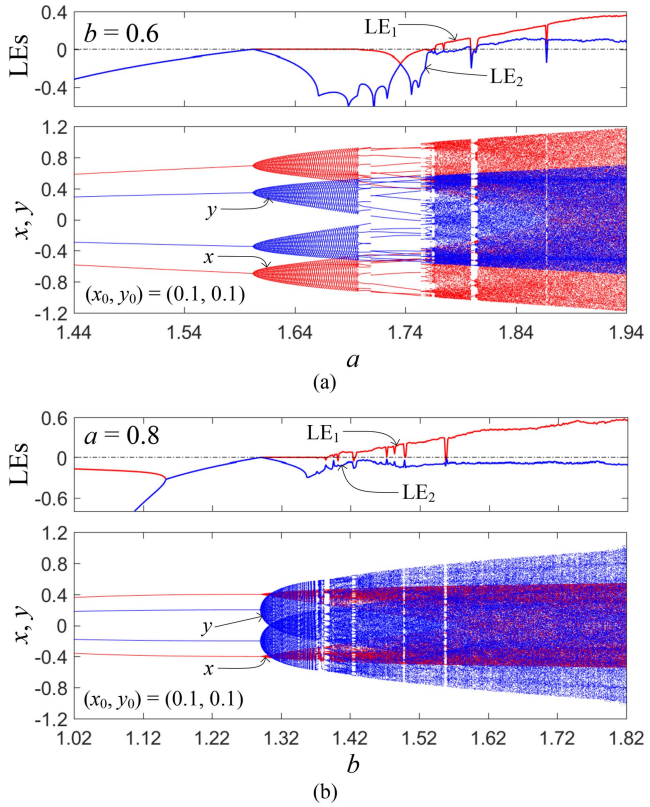

Fig. 4. 1-D mixed bifurcation plots consisting of bifurcation diagrams of state variables x, y (bottom) and two LEs (top), where the control parameters and initial states are marked in the figures. (a) Bifurcation plot for fixed $b = 0.6$. (b) Bifurcation plot for fixed $a = 0.8$.

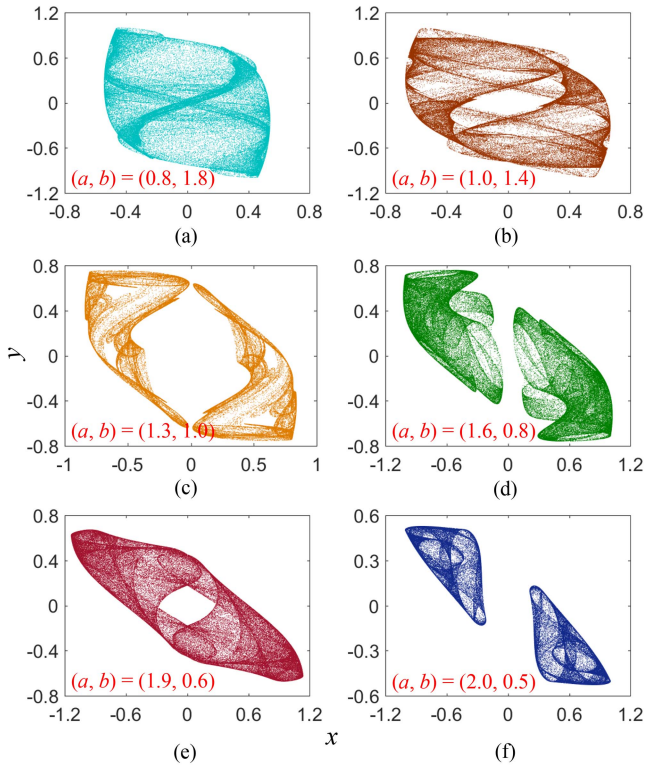

Fig. 5. Numerically simulated phase plane attractors of the 2-D STB memristive model under six sets of control parameters with fixed initial states $(x_0, y_0) = (0.1, 0.1)$. (a) $(a, b) = (0.8, 1.8)$. (b) $(a, b) = (1.0, 1.4)$. (c) $(a, b) = (1.3, 1.0)$. (d) $(a, b) = (1.6, 0.8)$. (e) $(a, b) = (1.9, 0.6)$. (f) $(a, b) = (2.0, 0.5)$.

in the 2-D STB memristive model. Consequently, the 2-D STB memristive model demonstrates complex dynamical behaviors, including stable point, period, multiperiod, quasi-period, chaos, hyperchaos, periodic window, and unbounded behavior.

Particularly, according to the critically stable interval of μ given in (11) and (12), we can roughly estimate the instability boundary in the $a - b$ parameter plane and derive the instability boundary equation as

$$L : b - 2/(\pi a) = 0. \tag{13}$$

This indicates that the motion trajectory initiated from $(x_0, y_0) = (0.1, 0.1)$ is stable if the condition $b - 2/(\pi a) < 0$ (i.e., $b < 2/(\pi a)$) is satisfied, resulting in the emergence of the stable point. The instability boundary described by (13) is also plotted in Fig. 3 using a white dotted curve, which almost overlaps the dividing line of the black and blue regions. The slight difference is caused by the critical eigenvalue $\lambda_1 = 1$ in (10).

To further exhibit the dynamical behaviors of the 2-D STB memristive model, we investigate its bifurcation behaviors related to the two control parameters.

When investigating the bifurcation behaviors of the 2-D STB memristive model, we set one of the control parameters a, b as a fixed value and set the other one as an alterable value. Fig. 4 shows the 1-D mixed bifurcation plots consisting of the bifurcation diagrams of state variables x, y and the two LE spectra. As illustrated in Fig. 4(a), when increasing a in the region [1.44, 1.94] and fixing $b = 0.6$, the 2-D STB memristive model shows the quasi-periodic bifurcation scenario and it displays hyperchaos within a wide parameter interval. As the control parameter a increases, the motion trajectory starts from period with two negative LEs, goes into quasi-period with zero maximal LE, turns into multiperiod with two negative LEs, then steps into chaos with one positive LE, and finally settles down hyperchaos with two positive LEs. As illustrated in Fig. 4(b), when increasing b in the region [1.02, 1.82] and fixing $a = 0.8$, the 2-D STB memristive model exhibits the same quasi-periodic bifurcation scenario but it only displays chaos within a wide parameter interval. As the control parameter b increases, the motion trajectory begins from period with two negative LEs, then enters into quasi-period with zero maximal LE, and directly settles down chaos with positive maximal LE. Besides, several narrow periodic windows with two negative LEs can be observed in the parameter intervals appearing chaos and hyperchaos.

B. Strange Attractors and Basins of Attraction

Six sets of control parameters are selected from different chaotic and hyperchaotic regions in Fig. 3. The phase plane attractors of the 2-D STB memristive model under these control parameter settings are obtained and the results in the $x - y$ plane are shown in Fig. 5. As can be viewed, these strange attractors have different complicated fractal structures, among which the strange attractors of Fig. 5(c), (d), and (f) have left/right fractal

TABLE I
LEs AND ATTRACTOR TYPES FOR SIX SETS OF CONTROL PARAMETERS

(a, b)	LE_1, LE_2	Attractor types
(0.8, 1.8)	0.5575, –0.0983	Solid chaotic attractor
(1.0, 1.4)	0.4280, –0.1213	Hollow chaotic attractor
(1.3, 1.0)	0.2767, –0.2090	Chaotic attractor with two pieces
(1.6, 0.8)	0.2465, 0.0366	Hyperchaotic attractor with two pieces
(1.9, 0.6)	0.3243, 0.0886	Hollow hyperchaotic attractor
(2.0, 0.5)	0.1705, 0.0369	Hyperchaotic attractor with two pieces

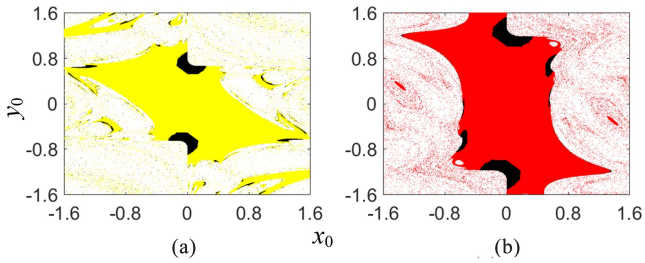

Fig. 6. Basins of attraction for two sets of control parameters. (a) Basin of attraction for $(a, b) = (1.9, 0.6)$. (b) Basin of attraction for $(a, b) = (0.8, 1.8)$.

structures. In addition, for these six control parameter settings, the two LEs and attractor types obtained from the 2-D STB memristive model are listed in Table I. As a result, the 2-D STB memristive model can exhibit various fantastic chaotic and hyperchaotic attractors related to these control parameter settings. In particular, for small control parameter a and large control parameter b, the proposed model is more likely to generate chaos with large maximal LE. However, for large a and small b, the memristive model is easier to generate hyperchaos with two positive LEs.

As demonstrated in Section II-B, the line fixed point appears in the 2-D STB memristive model and its stability depends on the control parameters and memristor initial state. Thus, the proposed memristive model can readily emerge the interesting phenomenon of multistability. To detect this phenomenon, we use a basin of attraction for the determined control parameters. The basin of attraction is painted by different colors to divide the initial state plane following the long-term motion trajectories of the proposed model.

For two control parameter settings, i.e., $(a, b) = (1.9, 0.6)$ and (0.8, 1.8), the basins of attraction are drawn by detecting every initial state in the $x_0 - y_0$ plane, and the results are depicted in Fig. 6(a) and (b). The yellow, red, and black regions represent hyperchaos (HC), chaos (CH), and stable point (SP), respectively. As can be seen, a hyperchaotic or chaotic attractor is coexisted with several stable points locating at different positions in the 2-D STB memristive model. According to the critically stable interval given in (12), there should be two stable point regions in the initial state plane for each control parameter setting. Since the two control parameter settings satisfy the condition that $b > 2/(\pi a)$, the critically stable intervals can be obtained from (12) as

$$\mu \in (-0.7746, -0.5147) \cup (0.5147, 0.7746) \quad (14)$$

TABLE II
PERFORMANCE OF CHAOTIC AND HYPERCHAOTIC SEQUENCES UNDER SIX CONTROL PARAMETER SETTINGS

(a, b)	ShanEn	PermEn	SampEn	CorDim	D_{KY}
(0.8, 1.8)	9.8633	**4.9800**	0.8041	1.5000	2.0000
(1.0, 1.4)	9.8661	4.6001	0.8067	1.4594	2.0000
(1.3, 1.0)	9.8423	3.6535	0.6920	1.4730	2.0000
(1.6, 0.8)	9.8248	4.0961	0.8064	1.6344	2.0000
(1.9, 0.6)	**9.9839**	3.8548	**1.0532**	**1.6402**	2.0000
(2.0, 0.5)	9.5826	3.6681	0.9944	1.4472	2.0000

The bold fonts indicate the best result among the column.

for $(a, b) = (1.9, 0.6)$ and

$$\mu \in (-1.3416, -1.0021) \cup (1.0021, 1.3416) \quad (15)$$

for $(a, b) = (0.8, 1.8)$. So, there are two large stable point regions that are symmetrical about the origin in each figure of Fig. 6. These numerical results basically accord with the theoretical expectations and their differences are caused by the critical eigenvalue $\lambda_1 = 1$ in (10).

Therefore, the phenomenon of multistability can be revealed in the 2-D STB memristive model. Besides, it can also be seen from Fig. 6 that the 2-D STB memristive model only presents hyperchaos or chaos in a relatively large region centered on the origin, indicating that the hyperchaos and chaos in these regions are robust about the initial states and have good ergodicity.

IV. PERFORMANCE ANALYSES FOR CHAOTIC/HYPERCHAOTIC SEQUENCES

This section evaluates the performance indicators of the chaotic/hyperchaotic sequences generated by the 2-D STB memristive model and compares them with the iterative sequences generated by six existing 2-D chaotic maps.

A. Chaotic/Hyperchaotic Sequences

From the generated chaotic/hyperchaotic attractors in Fig. 5, the corresponding iterative sequences can be generated. Using these control parameter settings in Fig. 5, six chaotic and hyperchaotic sequences with state variable x are generated and plotted in Fig. 7. All these iterative sequences are irregular and aperiodic. Thus, the proposed 2-D STB memristive model can be used to generate pseudorandom numbers (PRNs) for engineering applications.

B. Performance Evaluations

Using the control parameter settings given in Fig. 5, the chaotic/hyperchaotic sequences can be generated from the 2-D STB memristive model and their performance are evaluated using Shannon entropy (ShanEn), permutation entropy (PermEn), sample entropy (SampEn), correlation dimension (CorDim), and Kaplan–Yorke dimension (D_{KY}). The calculated performance indicators are listed in Table II, where the lengths of all these iterative sequences are set as 10^5. Note that the PermEn and D_{KY} indicators are calculated using the methods referring in [25].

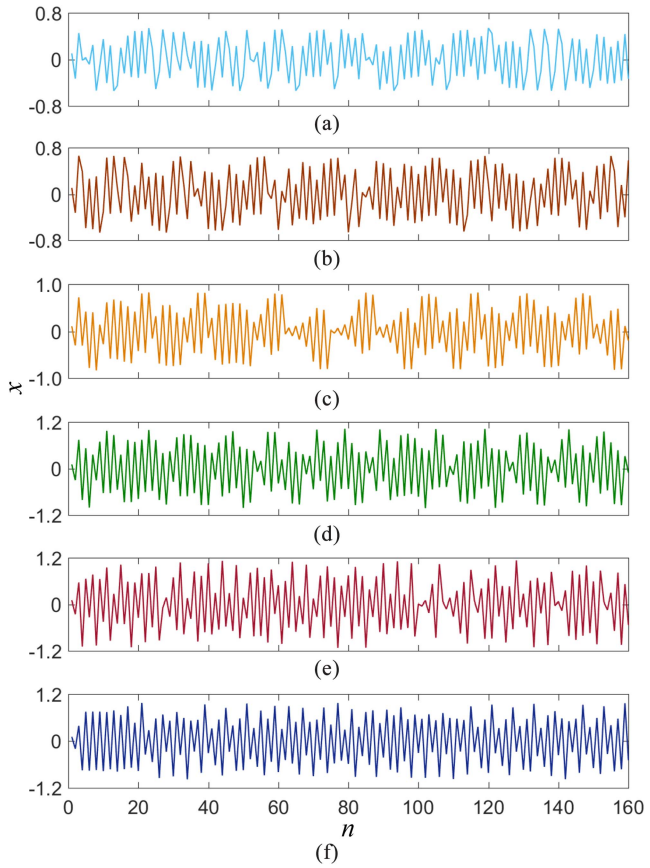

Fig. 7. Chaotic and hyperchaotic sequences generated from the 2-D STB memristive model under six sets of control parameters with fixed initial states $(x_0, y_0) = (0.1, 0.1)$. (a) $(a, b) = (0.8, 1.8)$. (b) $(a, b) = (1.0, 1.4)$. (c) $(a, b) = (1.3, 1.0)$. (d) $(a, b) = (1.6, 0.8)$. (e) $(a, b) = (1.9, 0.6)$. (f) $(a, b) = (2.0, 0.5)$.

The ShanEn is a widely used performance indicator to measure the random distribution of a signal [27]. To test the ShanEn of the chaotic sequences generated by different discrete maps, we design the experiments as follows for each map. First, a chaotic sequence of length 10^5 is generated. Second, the interval (0, 1) is equally divided into 2^{10} subintervals and the occurrence frequency of the chaotic sequence in each subinterval is counted. Finally, the ShanEn of the chaotic sequence is calculated. As can be seen from Table II, all the chaotic/hyperchaotic sequences generated by the 2-D STB memristive model have large ShanEn values. This illustrates that the 2-D STB memristive model has excellent ergodicity and its generated chaotic/hyperchaotic sequences are randomly distributed.

The SampEn is a performance indicator that can be used to evaluate the regularity of a chaotic sequence [28]. When using the SampEn to evaluate the regularity of a chaotic sequence, a larger SampEn indicates lower regularity of the chaotic sequence, and further means higher complexity of the related chaotic map. As can be seen from Table II, all the generated chaotic/hyperchaotic sequences have large SampEn values. This demonstrates the low regularity of chaotic/hyperchaotic sequences and the high complexity of the 2-D STB memristive model.

TABLE III
PERFORMANCE COMPARISONS FOR SOME 2-D MAP-BASED CHAOTIC SEQUENCES UNDER TYPICAL CONTROL PARAMETERS

Chaotic maps	Parameters	ShanEn	PermEn	SampEn	CorDim	D_{KY}
Proposed map	(1.9, 0.6)	**9.9839**	**3.8548**	**1.0532**	**1.6402**	**2.0000**
Q-DM map [25]	1.78	9.8792	3.4446	0.9489	1.5444	2.0000
Hénon map [30]	(1.4, 0.3)	9.7983	3.6501	0.8833	1.2107	1.2587
Lozi map [31]	(1.7, 0.5)	9.8304	3.8392	1.0177	1.3912	1.4046
NFI_a map [32]	–	8.4387	2.2066	0.1124	0.9826	1.1913
NEM_1 map [33]	2	8.7433	2.5012	0.3141	1.3248	1.4366
CF_a map [34]	(1.2, 2)	8.2285	2.9015	0.2827	1.1903	1.9783

The bold fonts indicate the best result among the column.

The CorDim is a class of fractal dimensions and depicts the dimensionality of the phase space occupied by a series of points [29]. It can be used to test the strangeness of a chaotic attractor. We calculate the CorDim values of the generated chaotic/hyperchaotic attractors using the calculation method in [29]. The results in Table II show that the generated chaotic/hyperchaotic attractors can achieve large CorDim values and, thus, occupy a high dimensionality in the phase space.

As a conclusion, the results in Table II show that all these generated chaotic/hyperchaotic sequences have excellent performance indicators. Obviously, with the control parameter setting $(a, b) = (1.9, 0.6)$, the 2-D STB memristive model has more excellent performance indicators than other control parameter settings.

C. Performance Comparisons

To compare the performance indicators of different 2-D chaotic maps, we take $(a, b) = (1.9, 0.6)$ as an example of control parameter setting for the 2-D STB memristive model, and set the control parameters of the six competing 2-D chaotic maps as the typical values reported in the original literature. These competing 2-D chaotic maps include the Q-DM map [25], Hénon map [30], Lozi map [31], hidden NFI_a map [32], NEM_1 quadratic map [33], and CF_a map with curve fixed points [34]. The initial state values of these 2-D chaotic maps are referenced to the settings given in [25].

Table III compares the ShanEn, PermEn, SampEn, CorDim, and D_{KY} of these 2-D chaotic maps. Note that from the perspective of the original literature, the performance indicators of the six competing 2-D chaotic maps can be considered optimal. Referring to Bao *et al.* [25] and Table III, it can be seen that only the 2-D STB memristive model and 2-D Q-DM map have two positive LEs, and thus they show hyperchaotic attractors with $D_{KY} = 2$. As a comparison, the other five 2-D chaotic maps have only one positive LE, and thus they display chaotic attractors with $D_{KY} < 2$. Similarly, the 2-D STB memristive model can achieve higher performance indicators than the six 2-D chaotic maps. This means that it has outstanding chaos complexity. These comparison results further verify the high randomness of the chaotic/hyperchaotic sequences generated by the 2-D STB memristive model.

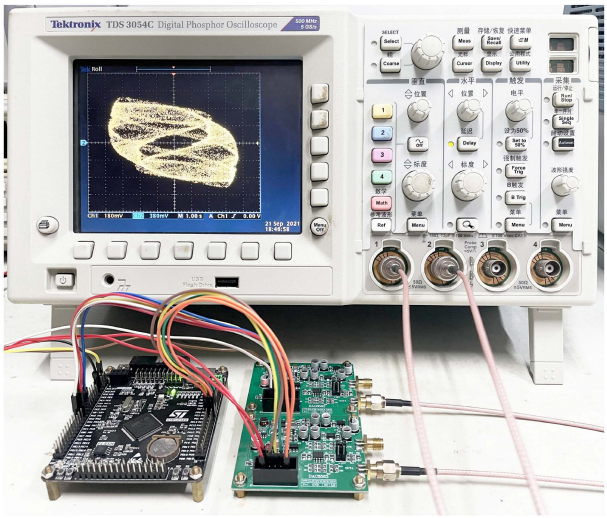

Fig. 8. Microcontroller-based digital hardware prototype and captured chaotic attractors generated by the 2-D STB memristive model.

V. Hardware Implementation and Application in PRNG

This section first develops a digital hardware prototype to implement the chaotic/hyperchaotic attractors generated by the 2-D STB memristive model, and then designs several PRNGs using the chaotic/hyperchaotic sequences acquired from the proposed model, as well as tests the randomness of these PRNGs.

A. Microcontroller-Based Hardware Experiments

A discrete mapping model is more suitable for digital hardware implementation than a continuous system model. To show the simplicity of hardware implementation, a digital hardware prototype of the 2-D STB memristive model is developed using a high-performance microcontroller. The STM32F407VET6 chip with ARM Cortex-M4 32-bit RISC core is selected as the microcontroller and the DAC8563 chip is taken as the D/A converter. The microcontroller is used for programming the 2-D STB memristive model and the D/A converter provides the analog voltage sequences. And then a level conversion circuit is designed to output the results to oscilloscope. Fig. 8 gives the snapshot of the digital hardware prototype.

The 2-D STB memristive model with the preset control parameters and initial states is programmed using C language and the software code is preloaded into the microcontroller. The six control parameter settings in Table I are used and the initial states are set as $(x_0, y_0) = (0.1, 0.1)$. When running the software code, the chaotic/hyperchaotic attractors under different control parameter settings can be acquired by the oscilloscope.

Corresponding to the numerically simulated phase plane attractors shown in Fig. 5, these chaotic/hyperchaotic attractors are experimentally acquired from the digital hardware prototype and their phase portraits are displayed in Fig. 9. In the acquired phase portraits, Ch1 and Ch2 are the x-channel and y-channel, respectively, and their labeled values are the scales of each division. To get a better view, the iterations of the 2-D STB memristive model are set to 2×10^5 and the time scale of the oscilloscope is tuned to 10 s. This ensures that more points can be acquired in each unit time. Afterward, following the

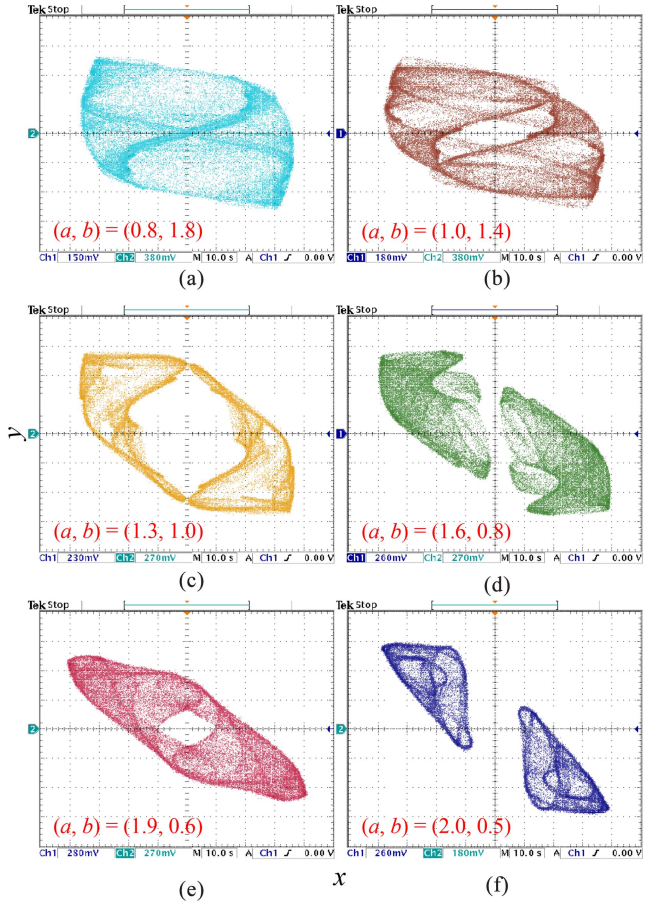

Fig. 9. Phase portraits of the chaotic/hyperchaotic attractors experimentally acquired from the digital hardware prototype under different control parameter settings. (a) $(a, b) = (0.8, 1.8)$. (b) $(a, b) = (1.0, 1.4)$. (c) $(a, b) = (1.3, 1.0)$. (d) $(a, b) = (1.6, 0.8)$. (e) $(a, b) = (1.9, 0.6)$. (f) $(a, b) = (2.0, 0.5)$.

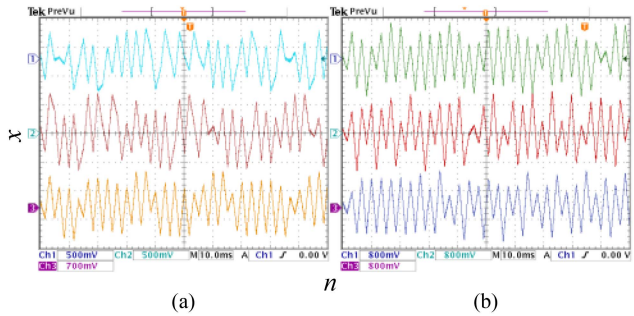

Fig. 10. Two groups of three-channel voltage sequences acquired from the digital hardware prototype under different control parameter settings. (a) First group of three-channel voltage sequences under $(a, b) = (0.8, 1.8)$ (top), (1.0, 1.4) (middle), and (1.3, 1.0) (bottom). (b) Second group of three-channel voltage sequences under $(a, b) = (1.6, 0.8)$ (top), (1.9, 0.6) (middle), and (2.0, 0.5) (bottom).

numerical chaotic/hyperchaotic sequences shown in Fig. 7, two groups of three-channel voltage sequences are experimentally obtained and shown in Fig. 10. Note that these experimental sequences are synchronously acquired from the digital hardware prototype of the 2-D STB memristive model under different control parameter settings. Hence, the experimental results in Figs. 9 and 10 are in accordance with the numerically simulated

ones and indicate the feasibility of the microcontroller-based hardware experiments.

B. Designed PRNGs and Randomness Analysis

Due to the characteristics of ergodicity, initial sensitivity, and unpredictability, chaotic systems are extensively applied to designing PRNGs [4]. In this section, we design six PRNGs using the 2-D STB memristive model under six control parameter settings and analyze the randomness of the generated PRNGs.

When designing a PRNG, the iterative sequence generated by a chaotic system can be directly used as the PRN. Denote $\{X(m)|m = 1, 2, \cdots\}$ as an iterative sequence generated by the 2-D STB memristive model. Each of $\{X(m)|m = 1, 2, \cdots\}$ is first converted to a 52-bit binary stream $\{X_B(m)|m = 1, 2, \cdots\}$ using IEEE 754 float standard. Thereafter, the digital numbers from 35th to 42th in $\{X_B(m)|m = 1, 2, \cdots\}$ are regarded as the PRNs. Thus, the generated PRNGs can be designed as

$$\text{PRNG} = X_B(m)_{35:42}. \tag{16}$$

Corresponding to the six chaotic/hyperchaotic sequences given in Fig. 7, each output from the 2-D STB memristive model can provide eight binary numbers. Therefore, six PRNGs are simply generated using the 2-D STB memristive model.

The TestU01 test suite is a strict and frequently used test standard for testing the randomness of PRNs and it provides several batteries of empirical statistical tests [35]. In our experiments, the five batteries, *Rabbit*, *Alphabit*, *BlockAlphabit*, *SmallCrush*, and *Crush*, are utilized to test the randomness of the designed PRNGs. These five batteries take different lengths of PRNs as inputs. The *Rabbit*, *Alphabit*, and *BlockAlphabit* can take 2^{32} bits as inputs and they contain 40, 17, and 102 empirical statistical tests, respectively. The *SmallCrush* takes about 6 Gb as input and has 15 empirical statistical tests. The *Crush* takes about 1 Tb as input and has 144 empirical statistical tests. To obtain fair test results, an open-source software TestU01[1] is used in experiments.

To prove the effectiveness of the generated PRNGs, the 2-D STB memristive model under six control parameter settings is separately used as the chaotic/hyperchaotic generators and the generated PRNGs are tested using the TestU01. The initial states for all the control parameter settings are set to $(x_0, y_0) = (0.1, 0.1)$. Table IV shows the TestU01 results of these six PRNGs using different lengths of PRNs as inputs. All these six PRNGs can pass all the empirical statistical tests. This indicates that the PRNGs generated by the 2-D STB memristive model have high randomness without chaos degradation when generating 1 Tb of PRNs.

To highlight the outstanding performance of the proposed 2-D STB memristive model, we compare its generated PRNGs with the PRNGs generated by the six competing 2-D chaotic maps in Table III using the TestU01. The control parameters and initial states for all the tested 2-D chaotic maps are set the same as the values used in Table III. The TestU01 results of these generated PRNGs with different lengths of PRNs are shown in Table V. As can be observed, the PRNGs generated by the Hénon

TABLE IV
TESTU01 RESULTS FOR DIFFERENT LENGTHS OF PRNS GENERATED BY THE 2-D STB MEMRISTIVE MODEL WITH SIX CONTROL PARAMETER SETTINGS

Control Parameters (a, b)	TestU01 Standard Test Suites*				
	Rabbit	*Alphabit*	*BlockAlphabit*	*SmallCrush*	*Crush*
	2^{32} bits			about 6 Gb	about 1 Tb
(0.8, 1.8)	40/40	17/17	102/102	15/15	144/144
(1.0, 1.4)	40/40	17/17	102/102	15/15	144/144
(1.3, 1.0)	40/40	17/17	102/102	15/15	144/144
(1.6, 0.8)	40/40	17/17	102/102	15/15	144/144
(1.9, 0.6)	40/40	17/17	102/102	15/15	144/144
(2.0, 0.5)	40/40	17/17	102/102	15/15	144/144

∗ The more detailed results by TestU01 Standard Test Suites are given on *https://github.com/charlesbao/STBMM_TestU01_Results*

TABLE V
TESTU01 RESULTS FOR DIFFERENT LENGTHS OF PRNS GENERATED BY SIX COMPETING 2-D CHAOTIC MAPS WITH TYPICAL CONTROL PARAMETERS

Chaotic maps	TestU01 Standard Test Suites*				
	Rabbit	*Alphabit*	*BlockAlphabit*	*SmallCrush*	*Crush*
	2^{32} bits			about 6 Gb	about 1 Tb
Q-DM map	12/40	4/17	8/102	**15/15**	15/144
Hénon map	**39/40**	**17/17**	**102/102**	**15/15**	**140/144**
Lozi map	32/40	15/17	98/102	13/15	123/144
NFI_a map	12/40	2/17	11/102	8/15	25/144
NEM_1 map	4/40	-	-	1/15	21/144
CF_a map	**39/40**	**17/17**	**102/102**	**15/15**	138/144

∗ The more detailed results by TestU01 Standard Test Suites are given on[2].
The bold fonts indicate the best result among the column.

and CF_a maps have relatively high randomness, but they fail to pass some empirical statistical tests in *Rabbit* test suite when the lengths of the tested PRNs reach to 2^{32} bits and in *Crush* test suite when the lengths reach to 1 Tb. However, the PRNGs generated by other competing 2-D chaotic maps have relatively low randomness and they fail to pass most empirical statistical tests. It should be noticed in particular that although the Q-DM map in [25] does have high conventional performance indicators, its generated PRNGs is prone to chaos degradation, whereas the newly proposed 2-D STB memristive model transformed from the Q-DM map does not occur chaos degradation, indicating that the proposed sine transform scheme is effective in enhancing chaos complexity to avoid chaos degradation. Therefore, the 2-D STB memristive model has outstanding performance and is more suitable for the application of PRNG.

VI. CONCLUSION

Both discrete memristor and sine transformation can enhance the chaos complexity of some existing discrete systems. In this article, we proposed a 2-D STB memristive model using the discrete memristor and sine transform scheme. Due to the line fixed point, the 2-D STB memristive model can demonstrate complex

[1][Online]. Available: http://simul.iro.umontreal.ca/testu01/tu01.html

[2][Online]. Available: https://github.com/charlesbao/STBMM_TestU01_Results

dynamical behaviors with quasi-periodic bifurcation and multistability. By setting different control parameters, the 2-D STB memristive model can emerge various chaotic and hyperchaotic attractors with complicated fractal structures and outstanding performance indicators. These advantages allow it suitable for chaos-based industrial applications. Furthermore, a digital hardware prototype was developed and these strange attractors were experimentally captured. Six PRNGs were designed using the proposed memristive model under different control parameter settings and the test results using the TestU01 showed that the generated PRNGs have high randomness without chaos degradation. In brief, the proposed 2-D STB memristive model has high flexibility in generating chaos and hyperchaos with high performance, and is suitable for many applications, such as secure video/RM-DCSK communication [18], [19]. In particular, the construction scheme for the 2-D STB memristive model can also be extended to other discrete memristors, which deserves further study.

REFERENCES

[1] Z. Hua, B. Zhou, and Y. Zhou, "Sine chaotification model for enhancing chaos and its hardware implementation," *IEEE Trans. Ind. Electron.*, vol. 66, no. 2, pp. 1273–1284, Feb. 2019.

[2] P. Z. Wieczorek and K. Gołofit, "True random number generator based on flip-flop resolve time instability boosted by random chaotic source," *IEEE Trans. Circuits Syst. I, Regular Papers*, vol. 65, no. 4, pp. 1279–1292, Apr. 2018.

[3] X. Meng, P. Rozycki, J.-F. Qiao, and B. M. Wilamowski, "Nonlinear system modeling using RBF networks for industrial application," *IEEE Trans. Ind. Informat.*, vol. 14, no. 3, pp. 931–940, Mar. 2018.

[4] M. Bakiri, C. Guyeux, J.-F. Couchot, L. Marangio, and S. Galatolo, "A hardware and secure pseudorandom generator for constrained devices," *IEEE Trans. Ind. Informat.*, vol. 14, no. 8, pp. 3754–3765, Aug. 2018.

[5] M. Chen, M. Sun, H. Bao, Y. Hu, and B. Bao, "Flux-charge analysis of two-memristor-based Chua's circuit: Dimensionality decreasing model for detecting extreme multistability," *IEEE Trans. Ind. Electron.*, vol. 67, no. 3, pp. 2197–2206, Mar. 2020.

[6] L. Chua, "If it's pinched it's a memristor," *Semicond. Sci. Technol.*, vol. 29, no. 10, Sep. 2014, Art. no. 104001.

[7] R. Ramamoorthy, K. Rajagopal, G. D. Leutcho, O. Krejcar, H. Namazi, and I. Hussain, "Multistable dynamics and control of a new 4D memristive chaotic Sprott B system," *Chaos Solitons Fractals*, vol. 156, Mar. 2022, Art. no. 111834.

[8] Y. Deng and Y. Li, "Symmetrical Hopf-induced bursting and hyperchaos control in memristor-based circuit," *Chaos*, vol. 31, no. 4, Apr. 2021, Art. no. 043103.

[9] M. Prezioso, F. Merrikh-Bayat, B. D. Hoskins, G. C. Adam, K. K. Likharev, and D. B. Strukov, "Training and operation of an integrated neuromorphic network based on metal-oxide memristor," *Nature*, vol. 521, no. 7550, pp. 61–64, May 2015.

[10] Q. Hong, H. Chen, J. Sun, and C. Wang, "Memristive circuit implementation of a self-repairing network based on biological astrocytes in robot application," *IEEE Trans. Neural Netw. Learn. Syst.*, to be published, doi: 10.1109/TNNLS.2020.3041624.

[11] S. Ergün, "On the security of chaos based 'true' random number generators," *IEICE Trans. Fundam. Electron. Commun. Comput. Sci.*, vol. 99, no. 1, pp. 363–369, 2016.

[12] H. Zhao, S. Gao, Z. He, X. Zeng, W. Jin, and T. Li, "Identification of nonlinear dynamic system using a novel recurrent wavelet neural network based on the pipelined architecture," *IEEE Trans. Ind. Electron.*, vol. 61, no. 8, pp. 4171–4182, Aug. 2014.

[13] M. Han, R. Zhang, T. Qiu, M. Xu, and W. Ren, "Multivariate chaotic time series prediction based on improved grey relational analysis," *IEEE Trans. Syst., Man, Cybern., Syst.*, vol. 49, no. 10, pp. 2144–2154, Oct. 2019.

[14] Z. Chen, X. Yuan, Y. Yuan, H. H.-C. Iu, and T. Fernando, "Parameter identification of chaotic and hyper-chaotic systems using synchronization-based parameter observer," *IEEE Trans. Circuits Syst. I, Regular Papers*, vol. 63, no. 9, pp. 1464–1475, Sep. 2016.

[15] E. Zeraoulia, *Robust Chaos and Its Applications*. Singapore: World Scientific, 2012.

[16] J. Zheng, H. Hu, and X. Xia, "Applications of symbolic dynamics in counteracting the dynamical degradation of digital chaos," *Nonlinear Dyn.*, vol. 94, no. 2, pp. 1535–1546, Oct. 2018.

[17] C. Li, D. Lin, J. Lü, and F. Hao, "Cryptanalyzing an image encryption algorithm based on autoblocking and electrocardiography," *IEEE MultiMedia*, vol. 25, no. 4, pp. 46–56, Oct.–Dec. 2018.

[18] S. Chen, S. Yu, J. Lü, G. Chen, and J. He, "Design and FPGA-based realization of a chaotic secure video communication system," *IEEE Trans. Circuits Syst. Video Technol.*, vol. 28, no. 9, pp. 2359–2371, Sep. 2018.

[19] H. Li, Z. Hua, H. Bao, L. Zhu, M. Chen, and B. Bao, "Two-dimensional memristive hyperchaotic maps and application in secure communication," *IEEE Trans. Ind. Electron.*, vol. 68, no. 10, pp. 9931–9940, Oct. 2021.

[20] B. Bao, K. Rong, H. Li, K. Li, Z. Hua, and X. Zhang, "Memristor-coupled logistic hyperchaotic map," *IEEE Trans. Circuits Syst. II, Express Briefs*, vol. 68, no. 8, pp. 2992–2996, Aug. 2021.

[21] Y. Deng and Y. Li, "Bifurcation and bursting oscillations in 2D non-autonomous discrete memristor-based hyperchaotic map," *Chaos Solitons Fractals*, vol. 150, Sep. 2021, Art. no. 111064.

[22] Z. Hua, Y. Zhou, and B. Bao, "Two-dimensional sine chaotification system with hardware implementation," *IEEE Trans. Ind. Informat.*, vol. 16, no. 2, pp. 887–897, Feb. 2020.

[23] H. Bao, Z. Hua, H. Li, M. Chen, and B. Bao, "Memristor-based hyperchaotic maps and application in AC-GANs," *IEEE Trans. Ind. Informat.*, to be published, doi: 10.1109/TII.2021.3119387.

[24] K. Li, H. Bao, H. Li, J. Ma, Z. Hua, and B. Bao, "Memristive Rulkov neuron model with magnetic induction effects," *IEEE Trans. Ind. Informat.*, vol. 18, no. 3, pp. 1726–1736, Mar. 2022.

[25] H. Bao, Z. Hua, H. Li, M. Chen, and B. Bao, "Discrete memristor hyperchaotic maps," *IEEE Trans. Circuits Syst. I, Regular Papers*, vol. 68, no. 11, pp. 4534–4544, Nov. 2021.

[26] Z. Hua, Y. Chen, H. Bao, and Y. Zhou, "Two-dimensional parametric polynomial chaotic system," *IEEE Trans. Syst., Man, Cybern., Syst.*, to be published, doi: 10.1109/TSMC.2021.3096967.

[27] J. Lin, "Divergence measures based on the Shannon entropy," *IEEE Trans. Inf. Theory*, vol. 37, no. 1, pp. 145–151, Jan. 1991.

[28] J. S. Richman and J. R. Moorman, "Physiological time-series analysis using approximate entropy and sample entropy," *Amer. J. Physiol. Heart Circulatory Physiol.*, vol. 278, no. 6, pp. H2039–H2049, Jun. 2000.

[29] A. M. Albano, J. Muench, C. Schwartz, A. I. Mees, and P. E. Rapp, "Singular-value decomposition and the Grassberger-Procaccia algorithm," *Phys. Rev. A*, vol. 38, no. 6, pp. 3017–3026, Sep. 1988.

[30] M. Hénon, "A two-dimensional mapping with a strange attractor," *Commun. Math. Phys.*, vol. 50, no. 1, pp. 69–77, Feb. 1976.

[31] V. Botella-Soler, J. M. Castelo, J. A. Oteo, and J. Ros, "Bifurcations in the Lozi map," *J. Phys. A, Math. Theor.*, vol. 44, Jun. 2011, Art. no. 305101.

[32] H. Jiang, Y. Liu, Z. Wei, and L. Zhang, "Hidden chaotic attractors in a class of two-dimensional maps," *Nonlinear Dyn.*, vol. 85, no. 4, pp. 2719–2727, Sep. 2016.

[33] S. Panahi, J. Sprott, and S. Jafari, "Two simplest quadratic chaotic maps without equilibrium," *Int. J. Bifurcation Chaos*, vol. 28, no. 12, Nov. 2018, Art. no. 1850144.

[34] H. Jiang, Y. Liu, Z. Wei, and L. Zhang, "A new class of two-dimensional chaotic maps with closed curve fixed points," *Int. J. Bifurcation Chaos*, vol. 29, no. 7, Jun. 2019, Art. no. 1950094.

[35] P. L'Ecuyer and R. Simard, "TestU01: A C library for empirical testing of random number generators," *ACM Trans. Math. Softw.*, vol. 33, no. 4, Aug. 2007, Art. no. 22.

Han Bao (Member, IEEE) received the B.S. degree in landscape design from the Jiangxi University of Finance and Economics, Nanchang, China, in 2015, the M.S. degree in art and design from Changzhou University, Changzhou, China, in 2018, and the Ph.D. degree in nonlinear system analysis and measurement technology from the Nanjing University of Aeronautics and Astronautics, Nanjing, China, in 2022.

In 2019, he visited the Computer Science Department, The University of Auckland, Auckland, New Zealand. He is currently a Lecturer with the School of Microelectronics and Control Engineering, Changzhou University. His research interests include memristive neuromorphic circuit, nonlinear circuits and systems, and artificial intelligence.

Houzhen Li (Graduate Student Member, IEEE) received the B.S. degree in optoelectronic information science and engineering from the Changshu Institute of Technology, Suzhou, China, in 2019. He is currently working toward the M.S. degree in electronics science and technology with the School of Microelectronics and Control Engineering, Changzhou University, Changzhou, China.

His research interests include memristive neuromorphic circuit and nonlinear circuits and systems.

Zhongyun Hua (Member, IEEE) received the B.S. degree in software engineering from Chongqing University, Chongqing, China, in 2011, and the M.S. and Ph.D. degrees in software engineering from the University of Macau, Macau, China, in 2013 and 2016, respectively.

He is currently an Associate Professor with the School of Computer Science and Technology, Harbin Institute of Technology, Shenzhen, Shenzhen, China. He currently serves as an Associate Editor for *International Journal of Bifurcation and Chaos*. His research interests include chaotic system, chaos-based applications, multimedia security, and data hiding.

Quan Xu (Member, IEEE) received the B.S. degree in physics from Huaiyin Normal University, Huaiyin, China, in 2005, and the Ph.D. degree in optical engineering from the University of Electronic Science and Technology of China, Chengdu, China, in 2011.

In 2018, he visited the Electrical Engineering and Electronics Department, The University of Liverpool, Liverpool, U.K. He is currently an Associate Professor with the School of Microelectronics and Control Engineering, Changzhou University, Changzhou, China. His research interests include memristor and memristive neuromorphic circuit.

Bocheng Bao (Member, IEEE) received the B.S. and M.S. degrees in electronic engineering from the University of Electronics Science and Technology of China, Chengdu, China, in 1986 and 1989, respectively, and the Ph.D. degree in information and communication engineering from the Nanjing University of Science and Technology, Nanjing, China, in 2010.

From 2008 to 2011, he was a Professor with the School of Electrical and Information Engineering, Jiangsu University of Technology, Changzhou, China. He was a Professor with the School of Microelectronics and Control Engineering, Changzhou University, Changzhou. In 2013, he visited the Department of Electrical and Computer Engineering, University of Calgary, Calgary, AB, Canada. His research interests include neuromorphic circuits, power electronic circuits, and nonlinear circuits and systems.

Dr. Bao was a recipient of the IET Premium Award in 2018 and selected as the Highly Cited Researcher 2021 and 2020 in Cross-Field.